Extremophiles (1997) 1:79–88

ORIGINAL PAPER

Rowan A. Grayling · Kathryn A. Bailey · John N. Reeve

DNA binding and nuclease protection by the HMf histones from the hyperthermophilic archaeon *Methanothermus fervidus*

Received: August 11, 1996 / Accepted: November 12, 1996

Abstract The DNA-binding and nuclease-protection properties of the HMf histones from the hyperthermophilic archaeon *Methanothermus fervidus* have been shown to be consistent with the formation of nucleosome-like structures (NLS). These proteins bind to DNA molecules as short as 20 bp and form complexes that protect DNA fragments from micrococcal nuclease (MNase) digestion that are 30 bp, ~60 bp and multiples of ~60 bp in length. The sequences of 49 of the ~60-bp DNA fragments protected from MNase digestion by HMfA have been determined and their intrinsic curvatures calculated. A circular permutation gel mobility-shift assay was used to determine directly the curvatures for five of these sequences. HMfA bound to intrinsically curved and noncurved DNAs, but exhibited a slight preference for the model curved DNA in binding competitions with a model noncurved DNA. The results obtained are consistent with the concept that the archaeal NLS is analogous, and possibly homologous, to the central core of the eukaryal nucleosome formed by a histone $(H3 + H4)_2$ tetramer.

Key words Nuclease protection · Nucleosomes · DNA-binding · Bent DNA · Gel mobility-shift assay

Although *Methanothermus fervidus* grows optimally at 83°C, the genome of this hyperthermophilic archaeon contains only 33 mol% G+C (Stetter et al. 1981), and therefore DNA-binding proteins are likely to contribute to the stability of this genome. Pursuit of this concept led to the discovery of HMf, a histone from *M. fervidus* (Sandman et al. 1990), that is now recognized as the archetype of a family of archaeal histones found in both methanogenic and nonmethanogenic *Euryarchaeota* (Grayling et al. 1994, 1996a,b). Preparations of HMf contain homodimers and heterodimers of two small (~7.5 kDa), basic (pI ~9) polypeptides, HMfA and HMfB, that have 85% identical amino acid sequences and sequences in common with the eukaryal nucleosome core histones (Sandman et al. 1990, 1994a). HMf is localized in the *M. fervidus* nucleoid (Bohrmann et al. 1994) and forms nucleosome-like structures (NLS) *in vitro* in which the DNA molecule is wrapped in a positive toroidal supercoil (Musgrave et al. 1991). These nucleoprotein complexes can be visualized directly by electron microscopy (Sandman et al. 1990; Howard et al. 1992) and their formation results in substantial DNA compaction that can be demonstrated and assayed easily by an agarose gel electrophoretic mobility-shift procedure (Sandman et al. 1990).

Nucleosome assembly in *Eukarya* is initiated by two histone H3–histone H4 dimers $[(H3 + H4)_2]$ binding to chromosomal DNA. Two histone H2A–histone H2B (H2A + H2B) dimers then attach to this central tetramer core to complete the histone octamer of the nucleosome (Arents and Moudrianakis 1991; Arents et al. 1993; Wolffe 1992). The location of the nucleosome is determined by the $(H3 + H4)_2$ tetramer which, in general, binds preferentially to DNA sequences with intrinsic curvature, usually designated as bent DNA sequences (Drew and Travers 1985; Satchwell et al. 1986; Thoma 1992). Eukaryal nucleosomes contain ~146 base pairs of DNA, wrapped ~1.8 times around the histone octamer in a negative toroidal supercoil (Wolffe 1992). However, the central $(H3 + H4)_2$ tetramer protects only ~73 base pairs of DNA from nuclease digestion (Dong and van Holde 1991) and may also wrap DNA in positive supercoils (Hamiche et al. 1996). Through their direct and indirect interactions with the transcription machinery, positioned nucleosomes play a major role in regulating eukaryal gene expression (Grunstein 1990; Kornberg and Lorch 1992; Travers and Schwabe 1993; Wolffe 1994).

Recently, a three-dimensional (3D) structure was established for the $(HMfB)_2$ dimer (Starich et al. 1996), and this confirmed the presence of the histone-fold motif that is conserved in all eukaryal core histones (Ramakrishman 1995). The conclusion that the HMf family of archaeal his-

Communicated by: G. Antranikian

R.A. Grayling · K.A. Bailey · J.N. Reeve (✉)
Department of Microbiology, The Ohio State University, Columbus, OH 43210, USA
Tel. +1-614-292-2301; Fax +1-614-292-8120
e-mail: reeve.2@osu.edu

tones and the eukaryal H2A, H2B, H3, and H4 histones evolved from a common ancestor, drawn previously from primary sequence comparisons (Sandman et al. 1990; Grayling et al. 1994), has therefore been substantiated at the 3D-structural level. Because of this homology, it seems likely that the HMf proteins also bind preferentially and assemble NLS-containing tetramer cores at intrinsically bent DNA sequences. HMf-containing NLS have been shown to localize at highly curved *Crithidia fasciculata* kinetoplast DNA fragments cloned into pBR322 (Howard et al. 1992). Here we report the sizes, sequences, and intrinsic curvatures of DNA molecules bound and protected from micrococcal nuclease (MNase) digestion by the HMf histones. These results provide evidence consistent with the archaeal NLS being analogous, and possibly homologous, to the DNA–protein complex formed by the eukaryal histone $(H3 + H4)_2$ tetramer.

Materials and methods

Microorganisms, plasmids, and protein preparations

M. fervidus cultures were grown, and HMf preparations were isolated from these cells as previously described (Sandman et al. 1994b; Grayling et al. 1996b). *E. coli* strain DH5α-F′ (Woodcock et al. 1989) was used for cloning, plasmid propagation, and to generate homogeneous preparations of recombinant (r) rHMfA and rHMfB (Sandman et al. 1994b; 1995). Plasmid DNAs were prepared by using CsCl gradients (Sambrook et al. 1989) or by a modified alkaline lysis method (Feliciello and Chinali 1993). The plasmids used as cloning vectors were pLITMUS28 (New England Biolabs, Beverly, MA, USA), pBR322, pUC19 (Yanisch-Perron et al. 1985), and pUC1318 that contains an inverted-repeat polylinker region (Kay and McPherson 1987). pBEND2 was used to assay for curved DNA sequences (Kim et al. 1989). pMS101 and pMM401, which contain the sequences $(5'TTTTTTGCCG)_{10}$ and $(5'AAAAAACGGCCCGGC)_5$, respectively, provided model curved $[(A_6N_4)_{11}]$ and noncurved $[(A_6N_9)_7]$ DNAs (Shimizu et al. 1995). Plasmid pRG101, constructed by ligating *Sma*I linearized pME2001, a methanogen-derived plasmid (Meile et al. 1983) into the *Sma*I site of pUC19, was used as the substrate DNA in most of the MNase protection experiments.

Preparations of purified HMf, rHMfA, and rHMfB were quantitated by amino acid analysis and stored as previously described (Grayling et al. 1995). Protein concentrations and molar ratios are given in terms of polypeptide monomers.

Micrococcal nuclease (MNase) digestion of HMf–DNA complexes

Linear DNA molecules were used to avoid variabilities in HMf–DNA interactions that might have resulted from differences in supercoiling in different plasmid DNA preparations. *Eco*RI-linearized pUC19 or *Sma*I-linearized pRG101 DNA (10 μg) was incubated with HMf, rHMfA, or rHMfB at 37°C for 20 min in 50 mM Tris-acetate (pH 8.8), 1 mM $CaCl_2$, 100 mM NaCl, in microfuge tubes pretreated with Sigmacote (Sigma, St. Louis, MO, USA) to prevent enzyme adsorption to the tube. MNase (0.01 U/ml; Sigma), diluted in 50 mM Tris-acetate buffer (pH 8.8) containing 100 mM NaCl, was added, incubation continued at 37°C for periods ranging from 30 s to 10 min, and the MNase activity was terminated by the addition of ethylenediaminetetraacetic acid (EDTA) (10 mM final concentration). The surviving DNA fragments were purified by phenol/chloroform extraction and ethanol precipitation (Sambrook et al. 1989), dried, redissolved in gel loading buffer [2% Ficoll (signa) 400, 10 mM EDTA (pH 8), 0.025% bromophenol blue] and visualized, by staining with 1 μg ethidium bromide (EtBr)/ml, following their separation by electrophoresis through either 8% total monomer (T), 3% cross-linker (C) containing polyacrylamide gels run using Tris-borate-EDTA buffer, or 4% NuSieve GTG agarose gels (FMC BioProducts, Rockland, ME, USA) run using Tris-acetate-EDTA buffer (Sambrook et al. 1989).

Southern blot analysis of MNase-protected fragments

The regional specificity of HMfA binding to pRG101 was investigated by Southern blot analyses of restriction fragments of pRG101 using [^{32}P]-labeled MNase-protected fragments of pRG101 as the probe. Following electrophoresis through 4% NuSieve GTG agarose gels, EtBr staining, and depurination using 0.25 M HCl, restriction fragments of pRG101 were transferred by overnight capillary alkaline transfer to Zetaprobe membranes (Bio-Rad Laboratories, Hercules, CA, USA). The membranes were used to generate Southern blots by hybridizations with ~30-bp and ~60-bp fragments of pRG101 that resulted from MNase digestion of rHMfA–pRG101 complexes. These fragments were purified from agarose gels and [^{32}P]-end-labeled using 5′ [α-^{32}P]-dATP and T4 polynucleotide kinase (Sambrook et al. 1989; Ausubel et al. 1990).

Cloning and sequencing of MNase protected fragments

A population of ~60-bp DNA fragments generated by MNase digestion of rHMfA–pRG101 complexes was end-filled using T4 DNA polymerase (Ausubel et al. 1990) and ligated with *Eco*RV-digested dephosphorylated pLITMUS28, and this ligation mixture was used to transform *E. coli* DH5α-F′. Plasmid preparations were isolated from ampicillin-resistant transformants and screened for insert DNAs by digestion at restriction sites that flanked the *Eco*RV site. Cloned DNAs were sequenced using Sequenase (USB, Cleveland, OH, USA), and the sequences obtained were analyzed using the GCG software (Genetics Computer Group, Madison, WI, USA).

Construction of pBEND2-60 plasmids

Five of the sequenced ~60-bp inserts were recloned from the pLITMUS28 constructs into pBEND2 (Kim et al. 1989; Zwieb et al. 1991) to test the computer predictions made for their intrinsic curvatures. The inserts were first PCR amplified from the pLITMUS28 clones using oligonucleotides with the sequences 5′-GTTTTCCCAGTCACGAC-3′ and 5′-AGCGGATAACAATTTCACACAGGA-3′ as primers. The PCR products were digested with *Eco*RI and *Bam*HI, end-filled using T4 DNA polymerase, and ligated with dephosphorylated *Hinc*II-digested pUC1318 which has *Xba*I sites flanking the *Hinc*II site. PCR amplification of the DNAs cloned into pUC1318, using the same primers, followed by *Xba*I digestion of the amplified products, generated *Xba*I fragments that were ligated with *Xba*I-digested dephosphorylated pBEND2 to generate five pBEND2-60 clones. The sequences of the insert DNAs cloned in these five pBEND2-60 plasmids were confirmed by resequencing.

Preparation of DNA substrates for the electrophoretic mobility-shift assays (EMSA)

The model DNA fragments $(A_6N_4)_{11}$ and $(A_6N_9)_7$ were released from pMS101 and pMM401 (Shimizu et al. 1995) by digestion with *Eco*RI and *Pst*I, and purified, following phenol–chloroform extraction, by electrophoresis through 8% polyacrylamide gels. These molecules were end-labeled with [α-^{32}P]-dATP by using the Klenow fragment of polymerase I to fill the *Eco*RI half-site.

DNA fragments, 18 bp and 21 bp in length, obtained by *Hae*III digestion of pBR322 were similarly purified and end-labeled with [γ-^{32}P]-ATP using T_4 polynucleotide kinase (Sambrook et al. 1989).

Electrophoretic mobility-shift assays (EMSA)

Aliquots (5 fmol) of ^{32}P-labeled $(A_6N_4)_{11}$ and $(A_6N_9)_7$ were incubated for 20 min at room temperature with increasing amounts of rHMfA in 10 µl reaction mixtures that contained 30 mM potassium 2′3′-cyclodiphosphoglycerate (Hensel and König 1988; Earle et al. 1996) and 50 mM Tris HCl (pH 8). Following the addition of 1 µl of a mixture of 50% glycerol, 0.4% bromophenol blue, and 0.4% xylene cyanol, the complexes formed were analyzed by electrophoresis through native 8% T 1.3% C polyacrylamide gels run at room temperature in 45 mM Tris-borate and 1 mM EDTA (pH 8), initially at 8 V/cm and then at 4.8 V/cm after the loading dyes had entered the gel. The gels were dried and the complexes visualized by autoradiography.

The same EMSA was used to evaluate the binding of rHMfA and rHMfB to the 18-bp and 21-bp DNA fragments of pBR322. Complexes were allowed to form in reaction mixtures that contained 70 pmol of the ^{32}P-labeled DNA fragments and increasing amounts of the histones.

DNA bend predictions and electrophoretic analysis

The shapes of DNA fragments were predicted as trajectories in three-dimensional space by the program AUGUR (Tan et al. 1988) with the ApA wedge model used to predict the helical parameters (bp roll and tilt, with a fixed twist angle) for each sequence as B-DNA (Ulanovsky and Trifonov 1987). AUGUR calculated a base-pair ratio (bp-ratio) and d_{max} from the curvature predicted for each sequence. The bp-ratio is the distance between the two ends of a DNA molecule in 3D space divided by the physical length of the molecule. The bp-ratio values generated were scaled to provide a comparative bending index, and indicate the overall degree of intrinsic curvature. The bp-ratios must be less than 1, except for a straight molecule which would have a bp-ratio of 1. A value of 0 on the comparative scale corresponds to a straight sequence, and a value of 100 would indicate a circular sequence.

The d_{max} is the longest distance between a base pair in the molecule and a straight line drawn to connect the ends of the DNA molecule, and indicates the extent of maximal *local* curvature. The d_{max} of a straight DNA molecule would be 0.

Local curvature predictions for the pRG101 sequence

The AUGUR software was used to calculate bp-ratio values for overlapping 60-bp sequences, staggered by 10-bp, along the entire length of pRG101. The values calculated were assigned to the central bp position of each 60-bp window, resulting in a local bending index at a 10-bp resolution, for each position on the pRG101 molecule. The 60-bp window was chosen to correspond with the mean size of the DNA fragments protected from MNase digestion by HMf binding.

Results

MNase digestion of HMf–DNA complexes

Eukaryal nucleosomes protect ~146 bp, and multiples of ~146 bp of DNA from MNase digestion, corresponding to the lengths of the DNA wrapped around individual and multiple adjacent nucleosomes (Noll 1974a,b; Thomas and Butler 1978; Wolffe 1992). MNase digestion studies were therefore undertaken to determine if the HMf proteins resembled the eukaryal histones in similarly protecting DNA molecules from MNase digestion, and protection of DNA fragments with discrete population sizes was observed (Fig. 1). MNase digestion of HMf–DNA complexes formed at protein/DNA molar ratios ≥200 resulted in DNA fragments that were multiples of ~60 bp which, with increasing digestion time, became a single population of ~60 bp fragments (Fig. 1a). Fragments ~30 bp in length were also generated at all stages of the digestion. The same profile of MNase-protected DNA fragments was generated with several different substrate DNAs and with preparations of na-

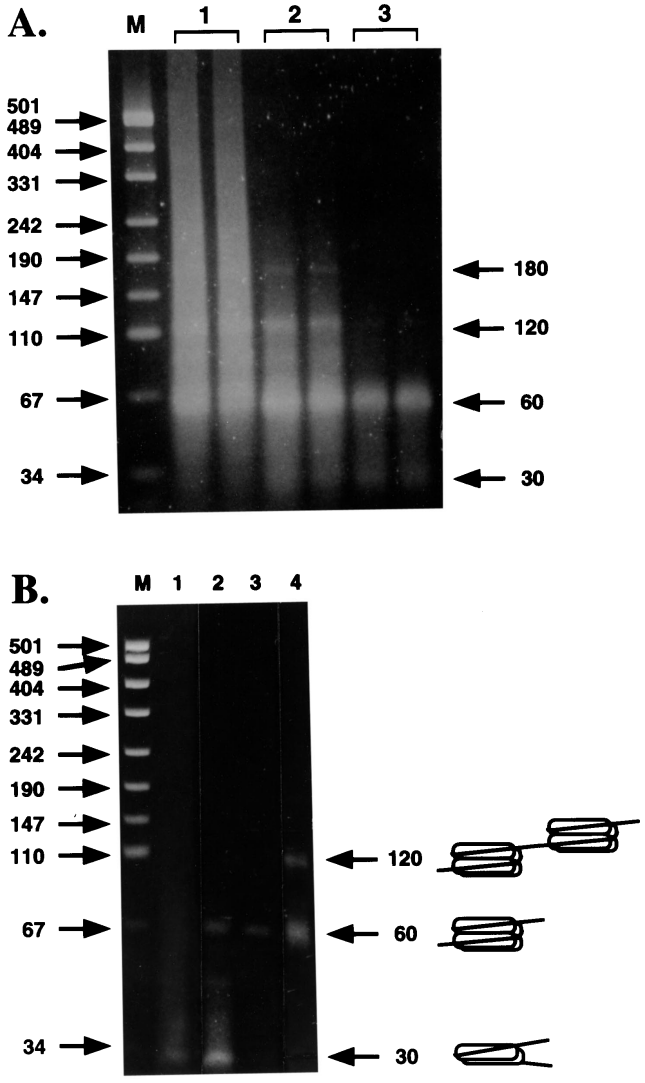

Fig. 1. Micrococcal nuclease (MNase) digestion of HMf–DNA complexes. **A** *Sma*I-linearized pRG101–HMf complexes formed at a protein/DNA molar ratio of 200 were exposed to MNase (0.25 mU/ml) for 3, 6, and 8 min. Duplicate samples of the MNase-protected DNA molecules were separated by electrophoresis through a 4% agarose gel in *tracks 1*, *2*, and *3*, respectively. Their approximate lengths (bp) indicated to the *right* of the figure. **B** *Eco*RI-linearized pUC19 DNA (10 μg) mixed with HMf at protein/DNA molar ratios of 0.2, 2, 20, and 200 was exposed to MNase (0.5 mU/ml) for 2 min (0.2, 2 ratios) or 10 min (20, 200 ratios). The approximate lengths of protected DNA fragments, separated by electrophoresis through an 8% total (T) 3% cross-linked (C) polyacrylamide gel, in *tracks 1–4* respectively, are indicated adjacent to diagrams that depict the protein/DNA complexes likely to be their origins (see text). *Msp*I fragments of pUC19 DNA were used as size standards (bp) (*tracks M*)

tive HMf, recombinant HMfA (HMfA), and recombinant HMfB (HMfB) (additional results not shown).

HMf molecules are polypeptide dimers in solution (Grayling et al. 1995) but, when bound to DNA at high protein/DNA molar ratios, they form tetramers (Grayling et al. 1996a). A model has therefore been developed which predicts that HMf dimers bind at low protein/DNA ratios and assemble into tetramer-containing DNA–protein complexes at higher protein/DNA ratios (Grayling et al. 1994, 1996a). MNase digestion of complexes formed at protein/DNA molar ratios of 0.2–2 resulted in MNase-protected fragments that were ~30 bp in length, but at higher protein/DNA ratios the protected fragments were predominantly ~60 bp in length and multiples of ~60 bp (Fig. 1b). This is consistent with the binding of an HMf dimer protecting ~30-bp DNA from MNase digestion, tetramers protecting ~60 bp, and adjacent tetramers protecting multiples of 60 bp.

Distribution of fragment sizes within an ~60-bp population

A population of ~60-bp fragments of pRG101 DNA, protected from MNase digestion by HMfA binding, was isolated from an agarose gel (Fig. 2b), [^{32}P]-end-labeled, and visualized by autoradiography following electrophoresis through a DNA-sequencing gel. The mean of the fragment size distribution was 59 ± 1 bp, and more than 90% of the fragments were between 52 bp and 67 bp in length (Fig. 2a).

Binding to short DNA molecules

Although the shortest DNA fragments detected as being protected from MNase digestion by the HMf proteins were ~30 bp in length, it was possible that these proteins could bind to even shorter DNA molecules. As demonstrated in Fig. 3, HMfA and HMfB did, in fact, bind and form stable complexes with a 21-bp DNA molecule and, to a lesser extent, with an 18-bp molecule.

Localized DNA binding by HMfA

To determine if HMfA binding exhibited a detectable preference for regions within the pRG101 molecule, ~30-bp and ~60-bp fragment populations protected from MNase digestion by HMfA binding to pRG101 were [^{32}P]-labeled and used as probes in Southern blot hybridizations against restriction enzyme digests of pRG101 DNA. Regions of the plasmid, over- or under-represented in the labeled populations, were expected to result in higher or lower than expected hybridization signals, respectively, and several restriction fragments exhibited anomalously low signals. This was unlikely to have resulted from unequal DNA transfer during the blotting procedure, as adjacent larger and smaller DNA fragments gave stronger autoradiographic signals (Fig. 4b). Almost the same non-stoichiometric band intensity patterns were obtained with the 30-bp and 60-bp probes, consistent with HMfA dimers binding and tetramers assembling at the same preferred locations.

Sequences of MNase-protected fragments

The binding specificity of HMfA to pRG101 DNA was investigated further by constructing a pLITMUS28 library

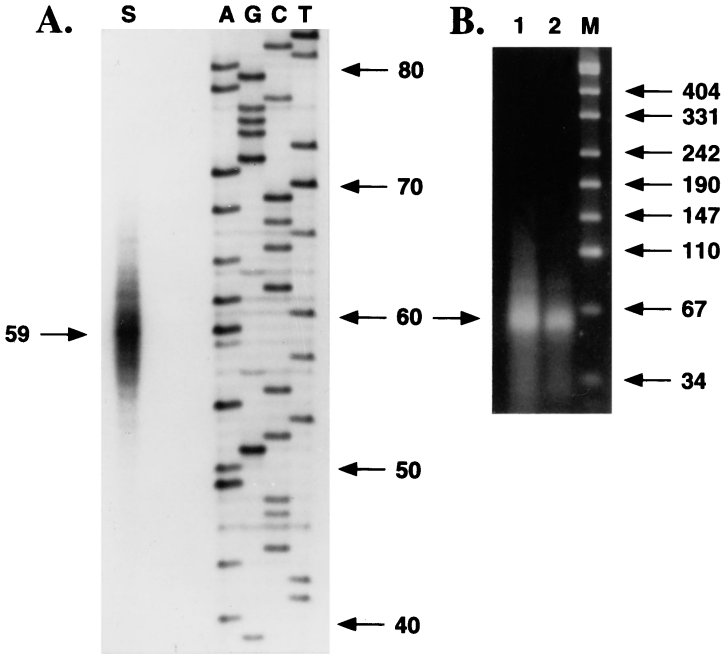

Fig. 2. Size distribution in a population of MNase-protected ~60-bp fragments. DNA molecules from the ~60-bp band indicated in *track 2* of **B** were [^{32}P]-end-labeled and separated by electrophoresis through a DNA-sequencing gel in *track S* of **A**. A sequencing ladder (*A*, *G*, *C*, *T*) provided size standards (bp). The center of the DNA fragment size distribution was 59 ± 1 bp, and more than 90% of the molecules were between 52 bp and 67 bp in length. The molecules in *tracks 1 and 2* of **B** were isolated from complexes of *Sma*I-linearized pRG101 DNA formed with HMfA at a protein/DNA molar ratio of 100 and digested with MNase (0.5 mU/ml) for 1 and 2 min, respectively. DNA size standards (bp) were separated in *track M*

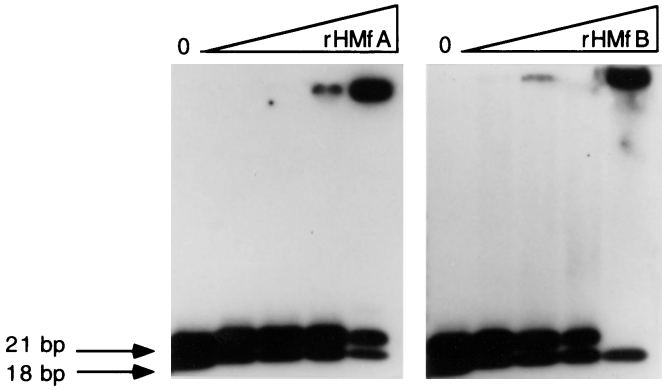

Fig. 3. Electrophoretic mobility-shift assays of HMfA and HMfB binding to 18-bp and 21-bp DNA fragments. Recombinant (*r*) *HMfA* or *HMfB* (3.3, 6.7, 13, and 40 μ*M*) was incubated for 20 min at 25°C with 70 pmol of the two ^{32}P-labeled DNA fragments, and the complexes formed were separated by electrophoresis at 4.8 V/cm through an 8% T 1.3% C native polyacrylamide gel and visualized by autoradiography. Control tracks (0) contained protein-free DNA fragments

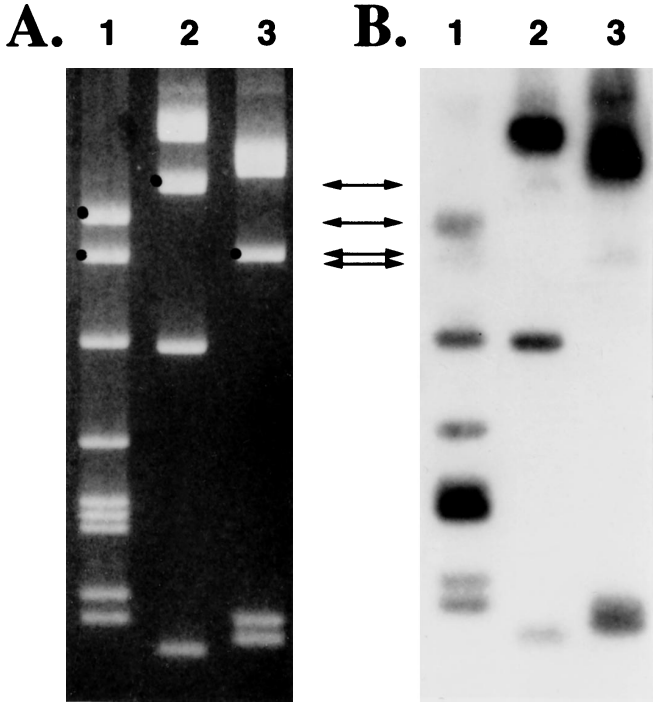

Fig. 4. Southern blot analysis of pRG101 restriction digests using [^{32}P]-labeled ~60-bp fragments as the probe. **A** Restriction digests of pRG101 generated by *Rsa*I, *Sty*I, and *Bam*HI plus *Eco*RI, separated by electrophoresis in *tracks 1–3*, respectively, of a 4% agarose gel. **B** The Southern blot obtained following the transfer of the fragments shown in a to a nylon membrane and hybridization with a population of ~60-bp DNA fragments, generated from pRG101–HMfA complexes by MNase digestion, and labeled with ^{32}P. Examples of restriction fragments with below-stoichiometric hybridization signals are identified by *dots* in **A**, and by *arrows* between the panels

of ~60-bp molecules that had been protected from MNase digestion by HMfA binding, and then sequencing these cloned DNAs. Of the 49 sequences obtained, 44 were different and, although several partially overlapped (Table 1), there were no clearly conserved primary sequence motifs. The mean size and range of sizes of the sequenced fragments were similar to those of the starting ~60-bp population (Fig. 2a), indicating that the pLITMUS28 library was representative of the original population of protected fragments.

Bp-ratio, d_{max} values, and bending indices were calculated using the AUGUR program (Tan et al. 1988) to facilitate comparisons of the intrinsic curvatures predicted for each sequence (Table 1). Fifteen sequences had bending

Table 1. Sequences and analysis of cloned ~60-bp DNA fragments, derived from micrococcal nuclease (MNase) digestion of rHMfA-protected pRG101

Clone[1]	Sequence	Cluster[3]	Length[4]	bp-ratio[5]	d_{max}[5]	Bending Index[5]
1, 2	CGATGTAACCCACTCGTGCACCCAACTGATCTTCAGCATCTTTTACTTTCACCAGCGTTTCTGGGTGAGCAAAAACAGGA	5	80	0.96	18.9	4
3	TCCTCAAATCCCTACCAGAATACTCTGATGAGTTATATAAACAGCATACTAATTCAATCT	2	60	0.94	23.5	6
4	ATTCCATCTACCTGGGGTGTCATCCCCCACTATGGGGTTGTGTTTTTCTGTGGTTTTGTGTGT	4	63	0.94	27.4	6
5	ACTGCAGGATTTAAGGGTTGAATCCCTCAAGACTGGTAGGTTTGTGTCTGTTGGGTGTGTCATGAGGGATGCCCT		75	0.77	69.7	23
6	ACTCGACCTGAGAGGGTATAGTAACAGGGACATCAAGCACATAGTTGGACTTGTGAAGGCCGTGACATGGTACAGGCAACAT	2	82	0.95	35.4	5
7	AAAAATAGGCGTATCACGAGGCCCTTTCGTCTCGCGCGTTTCGGTGATGACGGTGAAAACCTCTGA		66	0.92	32.2	8
8	TCCTGTCTGAGAAAGCAAAAAAATACAAGAAAATCCGTGGA	4	41	0.93	21.3	7
9	ACGCTCAGTGGAACGAAAACTCACGTTAAGGGATTTTGGTCATGAGATTATCAAAAAGGATCTTCACCT		69	0.89	38.1	11
10a[2]	GGGGATCCTCTAGAGTCGACCTGCAGGCATGCAAGCTTGGC		41	0.99	7.2	1
10b[2]	CCCAGTCACGACGTTGTAAAACGACGGCCAGTG		33	0.95	14.7	5
11	ACCTCGCACCCCTCGGGAGGGATCCGAATACAAAGGAATTCACAGATGAACTCCACCACCTCT	3	63	0.98	14.7	2
12	TGAGAATAGTGTATGCGGCGACCGAGTTGCTCTTGCCCGGCGTCAATACGGGATAATACCGCGCCACATAGCA	5	73	0.95	33.5	5
13	AGCACATCCTCCTCGCAGGTGAGGTGCTCCACCCAGGAGGGGATGTTATTGAACCCCAATCATTC	1	65	0.98	9.1	2
14	AGGCCGTGACATGGTACAGGCAACATAAAAGGAGGAGGGAGGGGAGTTATGTCCGTGAAGGTGGCCATGACATTATCATCGGCACTGA GGATGACCTGAGGGATGCATTGGAGT	2	114	0.98	18.3	2
15	AGCAAAAAAATACAAGAAAATCCGTGGATGACTCCATTATGAATCTATTTTGAATCCGTCT	4	61	0.85	40.9	15
16	CCTGACGAGCATCACAAAAATCGACGCTCAAGTCAGAGGTGGCGAAACCCGACAGGACTATAAAGATACCAGGCGT	4	76	0.95	22.5	5
17, 18	TGATCATTACAGGCTCATCCTCGGCCCTGCAGGTGAGGAGTATGTTCGGCTGTCATCACGGGTTAAGGT	3	69	0.96	27.5	4
19, 20	TGGTGTGGGTGGTGATCTGCAGGCTGAGTACACTGATGCAATGGCACGGGGTGATGACTCG		61	0.96	20.8	4
21, 22	TGTAAATATCTATATCCTCCATGGATTAATAATTTTGGGAATTTTGGGAGGGTTGAACCACCACCCT	4	67	0.79	60.3	21
23	TGGGTTCCCCTATAATCAAGTCCTGTCTGAGAAAGCA		37	0.98	8.3	2
24	AAGCCTACGCTGACCAGTTAATCAATGATGACAGCATCGACATCCTCGAATCCATCACCAGAGTCATAGGGGAGGCCCATTATGGT	1	87	0.92	44.5	8
25	TGCCGGGAGCAGACAAGCCCGTCAGGGCGCGTCAGCGGGTGTTGGCGGGTGTCGGGGCTGGCTTAACT		69	0.98	11.1	2
26	TGAAGCCTGGTGACCTCCTGGTGGTGGAGA		30	0.98	7.9	2
27	TGCTACAGGCATCGTGGTGTCACGCTCGTCGTTTGGTATGGCTTCATTCAGCTCCGGTTCCCAACGA		67	0.95	31.0	5
28	TGATGTCAGGGTTTACAACCCCTACCTCCACCTACTCGACCTGAGAGGGTATAGTAACAGGGACATCAAGCACATAGTTGGACTTGTG AAGGCCGTGACATGGTACAGGCAACATAAAAGGAGGAGGGAGGGGAGTTATGTCCG	1	145	0.94	55.4	6
29	TCCAAATCACCAAAGCCTTCAAGTAACCCCTTAAGGTCTTCAGGTTTGAACTCTGGGATGTCATCAAGGT		71	0.94	32.2	6
30	TAAGAGGATCATGGAGGCCTACGAGGTCATCAGGGCTGTCTATGAGCGATTGA	2	54	0.96	17.6	4
31	CTGTAAGCGGATGCCGGGAGCAGACAAGCCCGTCAGGGCGCGTCAGCGGGTGTTGGCGGGTGTCGGGGCTGGCT		75	0.98	9.5	2
32	ACAAGCCTACGCTGACCAGTTAATCAATGATGACAGCATCGACATCCTCGA	1	52	0.97	13.4	3
33	CGTTCATCCATAGTTGCCTGACTCCCCGTCGTGTAGATAACTACGAT		48	0.98	8.2	2
34a[2]	AGTCACGACGTTGTAAAACGACGGCCAGTG		32	0.96	16.7	4
34b[2]	GGGGATCCTCTAGAGTCGACCTGCAGGCATGCAAGCTTGG		42	1.00	0.2	0
35	TCCAACCCGGTAAGACACGACTTATCGCCACTGGCAGCAGCCACTGGTA		50	0.98	5.7	2
36	TGTTGACATGGACTTGGGAACAGCGGAAAATGCTCGGATTTGGAAAAAAACCATATTCCATAGTATGGT		69	0.82	57.6	18
37, 38	TCGAGTATGCGAAGGAATTGGGTGAGGTTCGGCGGGAGATAGAGGATATGCAGGGGGGGTGATCCA	3	66	0.98	13.0	2
39	AGCACATAGTTGGACTTGTGAAGGCCGTGACATGGTACAGGCAACATAAAAGGAGGAGGGAGGGGAGT	2	69	0.97	18.4	3
40	AGCACATCCTCCTCGCAGGTGAGGTGCTCCACCCAGGAGGGGATGTTATTGAACCCCAATCAT	1	64	0.98	8.6	2
41	CAGCGTTTCTGGGTGAGCAAAAACAGGAAGGCAAAATGCCGCAAAAAAGGGAATAAGGGCGACACGGA	5	68	0.85	47.3	15
42	TGGAAACAGGTGGAGAATCCTCCAATCACGGAGATAAGCATGATTTGGTGTTGACCAGGGCCGGG		66	0.97	10.2	3
43	TGAAAAAGCGTTGTTGAGTGGGGTGGAAATACCGCACACCAAAACCCCACCAACACAGTCACCCTG		68	0.94	27.9	6
44	AGGCGTTTCCCCCTGGAAGCTCCCTCGTGCGCTCTCCTGTTCCGACCCTGCCGCTTACCGGAT		64	0.96	23.0	4
45	TGTCATGCCATCCGTAAGATGCTTTTCTGTGACTGGTGAGTACTCAACCAA	5	52	0.96	17.0	4
46	ACATCCTCCTCGCAGGTGAGGTGCTCCACCCAGGAGGGGATGTTATTGAACCCCAATCA		60	0.98	7.7	2
47	ACGTTCTTCGGGGCGAAAACTCTCAAGGATCTTACCGCTGTTGAGATCCAGTTCGATGTAACCCACTCGTGCA	5	74	0.91	36.5	9

[1] ~60-bp fragments cloned from a population of molecules protected from MNase digestion by HMfA, as described in Fig. 2.
[2] Sequences a and b are from separate locations in pRG101 and therefore must have been ligated and cloned coincidentally together in these plasmids.
[3] Cluster numbers as designated in Fig. 5.
[4] Lengths of the cloned sequences in base pairs. The mean length of the sequenced fragments was 64 bp.
[5] Bp-ratio, d_{max}, and bending index are the curvature parameters predicted for each sequence by the AUGUR software. Molecules with substantial intrinsic curvatures have bending indices ≥5 (Tan et al. 1988).

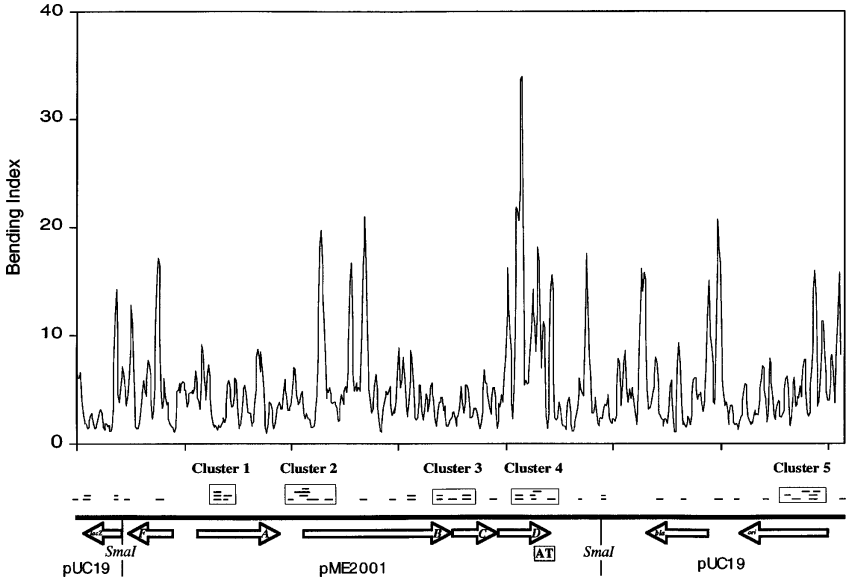

Fig. 5. Summary of the results of cloning and sequencing ~60-bp DNA fragments. The locations of the sequences in Table 1 are indicated by the *short horizontal lines above the map* of the pRG101 plasmid (*long, thick horizontal line*). The local bending index for the pRG101 sequence at a 10-bp resolution is shown in the graph (*ordinate scale* of 1 kbp) *above* the pRG101 map. Sequences within 100 bp of each other are *boxed* and designated as *clusters*. pRG101 is 7125 bp in length and was constructed by ligating *Sma*I-linearized pME2001 (Meile et al. 1983) into the *Sma*I site of pUC19. *Open arrows* identify *open reading frames A–D* in pME2001, and genetic loci in pUC19 (*lacZ*, *bla*, *ori*). An A/T-rich region (*AT*), possibly the pME2001 origin of replication (Nölling 1992) is boxed

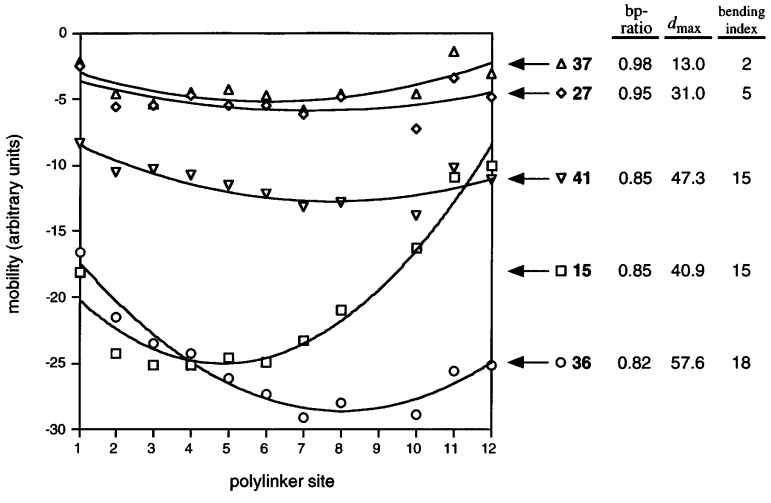

Fig. 6. Circular permutation gel mobility assays (CPMA) of pBEND2-60 inserts. pBEND2-60 plasmid DNAs containing the insert sequences 15, 27, 36, 37, and 41 (Table 1) were digested with restriction enzymes that cleaved at the polylinker sites 1–8 and 10–12. Cleavage at site 5 positioned the insert at the center of the released fragment, whereas cleavage at sites 1 and 12 positioned the insert at either end of the fragment. Following electrophoresis through 10% T 1.3% C polyacrylamide gels, the mobilities of the released DNA fragments were determined relative to the mobility of the equivalent pBEND2 polylinker fragment that lacked an ~60-bp insert. The relative mobilities are plotted against the position of the polylinker restriction site and are fitted with *lines* that are 2nd-order least-squares fits to the mobility data. Released DNA fragments from plasmids with insert sequence 15 are shown with *squares*; 27, *diamonds*; 36, *circles*; 37, *triangles*; and 41, *inverted triangles*. d_{max}, extent of maximum local curvature

indices greater than 5, indicative of substantial intrinsic curvature, whereas the remainder had lower bending indices consistent with very little intrinsic curvature. The locations of the sequenced fragments within the pRG101 molecule are shown in Fig. 5, together with the bending index that was calculated for overlapping 60-bp sequences, at 10-bp intervals, along the pRG101 molecule. Twenty-three of the sequenced fragments fell into five clusters, some of which had overlapping sequences and all of which were within 100 bp of each other (Fig. 5). Clusters 2, 4, and 5 are in regions of the pRG101 molecule predicted to be highly curved, whereas clusters 1 and 3 are in regions not predicted to have significant intrinsic curvature.

Experimental evaluation of predicted curvatures

To evaluate the predictions of the AUGUR software, five of the sequenced fragments were analyzed by a circular permutation gel mobility assay (CPMA). These were chosen as representatives of ~60-bp fragments predicted to be curved (clones 15, 36, and 41), noncurved (clones 27 and 37), members of clusters (clones 15, 37, and 41), and nonclustered sequences (clones 27 and 36). They ranged in lengths from 61 to 69 bp (Table 1). The DNA fragments were inserted into the *Xba*I site of pBEND2 which is flanked by direct repeats of a sequence that contains multiple restriction sites. Cleavage at the different flanking sites therefore released the same sized fragment, but with the cloned sequence of interest at different positions relative to the ends of the fragment (Kim et al. 1989). The relative electrophoretic mobilities of the DNA fragments released by the different restriction enzymes are plotted against the position of each restriction enzyme site in the flanking polylinker sequence (Fig. 6). Fits with a second-order polynomial function are shown for the data points obtained.

Bent sequences reduce the electrophoretic mobility of a linear DNA molecule most when positioned near the center of the molecule. Such sequences are therefore revealed by parabolic fits to the CPMA data that have deep minima, whereas nonbent sequences give almost flat fitted curves

(Kim et al. 1989). As shown in Fig. 6, two of the sequences predicted by the AUGUR software to be intrinsically curved (clones 15 and 36) exhibited electrophoretic mobilities in the CPMA consistent with substantial intrinsic curvature, and the two predicted to be straight (clones 27 and 37) had mobilities indicative of little if any intrinsic curvature. There was not, however, complete consistency between the curvature predictions and experimental results. The fragments of DNA released from the pBEND-60 clone that contained sequence 41, a sequence predicted to be curved, did not migrate as expected for substantially curved DNAs.

HMf binding to curved and noncurved DNA molecules

Although the evidence from regional binding and from sequencing of protected fragments indicated that HMfA bound to some but not all of the possible ~60-bp sequences within the pRG101 molecule, this included both curved and noncurved DNA sequences (Table 1). HMfA binding to model sequences designed to be curved $[(A_6N_4)_{11}]$ and noncurved $[(A_6N_9)_7]$ (Shimizu et al. 1995) was therefore investigated directly. These sequences have approximately the same lengths and base composition but the A_6 tract is in phase with the 10·4-bp helical repeat of the DNA in the $(A_6N_4)_{11}$ sequence, which is therefore highly curved, whereas the A_6 tract is out of phase with the helical repeat in the $(A_6N_9)_7$ sequence, which is therefore not curved but rather has a zigzag configuration. When HMfA was added to an equimolar mixture of these two DNAs, binding occurred preferentially to the curved molecule at the lowest protein/DNA ratio, but at higher ratios, HMfA bound and formed stable complexes with both DNAs (Fig. 7). As expected, despite their similar lengths, when protein-free these DNA molecules had very different electrophoretic mobilities. This was also the case for the complexes formed with HMfA at the lowest protein/DNA ratios (complexes designated Ia and Ib in Fig. 7), but at higher protein/DNA ratios, the complexes that formed (IIa/IIb and IIIa/IIIb) had very similar mobilities, indicating that the original shape of the DNA molecule no longer played a dominant role in determining the electrophoretic mobilities. As the protein/DNA ratio was increased, complexes Ia and Ib disappeared, consistent with complexes that contained HMfA dimers being assembled into complexes IIa/IIb and IIIa/IIIb that contained tetramers.

Discussion

The discovery of the HMf proteins in *M. fervidus* (Sandman et al. 1990) and their close relatives HPy and HAN1 in *Pyrococcus* and *Thermococcus* species (Sandman et al. 1994a; Rominus and Musgrave 1996) fulfilled the expectation that DNA-binding proteins would be abundant in hyperthermophilic *Archaea*. However, the recognition that these proteins are histones and that members of this family of proteins are also present in mesophilic *Archaea* (Darcy et al. 1995), has now focused attention on the premise that histones evolved in a common ancestor of the *Archaea* and *Eukarya*, and that the highly conserved structure of the modern eukaryal nucleosome has evolved from a simpler structure that may still exist in *Archaea*.

The results reported here are consistent with this idea. DNA binding by the HMf histones, shown by electron microscopy to result in structures that visibly resemble nucleosomes (Sandman et al. 1990; Howard et al. 1992), has now been shown to protect DNA molecules from nuclease digestion and to generate populations of protected fragments that are consistent with the formation of nucleosome-like structures (NLS; Fig. 1). Eukaryal nucleosomes protect ~146-bp from nuclease digestion (Wolffe 1992), but the central core of a nucleosome formed by a $(H3 + H4)_2$ histone tetramer protects only ~73-bp (Dong and van Holde 1991). The complexes formed by the smaller HMf proteins protect ~60-bp (Fig. 1) which, together with the observation that HMf molecules are cross-linked into tetramers when bound to DNA, is consistent with the proposal that archaeal NLS have a tetramer core (Grayling et al. 1994, 1996a,b). Nucleosomes are positioned by the $(H3 + H4)_2$ histone tetramer (Dong and van Holde 1991; Hayes et al. 1991; Pruss and Wolffe 1993) which apparently recognizes inherent shape and the flexibility of a DNA sequence as positioning information (Drew and Travers 1985; Crothers et al. 1991; Thoma 1992). These parameters deter-

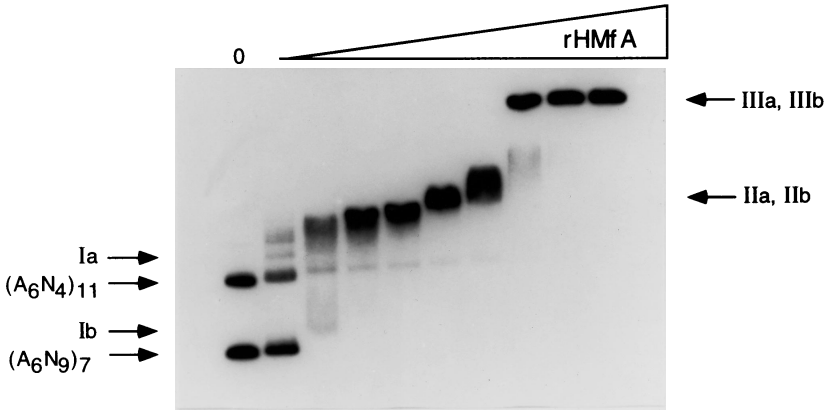

Fig. 7. Electrophoretic mobility-shift assays of rHMfA binding to curved $(A_6N_4)_{11}$ and noncurved $(A_6N_9)_7$ DNA molecules. A mixture of 5 fmol of each of the two [^{32}P]-labelled DNAs was incubated with HMfA (0.3, 0.67, 1.0, 1.3, 1.9, 3.3, 6.7, 10, and 13 μM) for 20 min at 25°C. Complexes formed with the curved DNA (*Ia*, *IIa*, and *IIIa*) and with the noncurved DNA (*Ib*, *IIb*, and *IIIb*) were separated by electrophoresis at 4.8 V/cm through a native 8% T, 1.3% C polyacrylamide gel and visualized by autoradiography. The control track (O) contained protein-free DNA molecules

mine where nucleosomes assemble and which side of the double helix faces inward and which side faces outward. Although the precise rules that govern nucleosome positioning remain to be determined (Thoma 1992), nucleosome localization clearly plays a major role in regulating eukaryal gene expression (Grunstein 1990; Kornberg and Lorch 1992; Wolffe 1994) and this does involve the preferential binding of the $(H3 + H4)_2$ histone tetramer to a sequence-determined DNA shape (Pruss and Wolffe 1993). Wrapping and constraining a DNA molecule around a nucleosome should be energetically less costly, and nucleosome assembly is therefore generally favored at DNA sequences that are inherently curved (Thoma 1992). The formation of HMf containing NLS should similarly be facilitated by inherently curved and flexible DNA sequences, and, although there were no obviously conserved primary sequence motifs in the fragments of pRG101 protected from MNase digestion by HMfA binding (Table 1), evidence was obtained for regional localization of NLS on the pRG101 molecule (Figs. 2, 5). Several of the pRG101 sequences protected from MNase digestion by HMfA were predicted (Table 1), and two were demonstrated directly to be intrinsically curved (Fig. 6). These were not, however, the majority of the sequences and although HMfA did exhibit a slight binding preference for the model curved $(A_6N_4)_{11}$ DNA sequence, complexes were also readily formed with the noncurved $(A_6N_9)_7$ sequence (Fig. 7). Some DNA sequences are known to exert a very dominant effect on nucleosome positioning (Pruss and Wolffe 1993; Godde and Wolffe 1996) but, in most situations, the intrinsic shape of the DNA is unlikely to be the only positioning parameter. Local variations in superhelicity, transcription and replication also participate in nucleosome assembly, disassembly, and positioning (Wolffe 1992), and these parameters presumably must also play roles in determining when and where NLS assemble in *Archaea*.

Acknowledgments This work was supported by NIH grant GM53185. We thank N.D. Priestly and M. Shimizu for gifts of the cyclic diphosphoglycerate, and plasmids pMM101 and pMS401, respectively.

References

Arents G, Moudrianakis EN (1993) Topography of the histone octamer surface: repeating structural motifs utilized in the docking of nucleosomal DNA. Proc Natl Acad Sci USA 90:10489–10493

Arents G, Burlingame RW, Wang B-C, Love WE, Moudrianakis EN (1991) The nucleosomal core histone octamer at 3.1 Å resolution: a tripartite protein assembly and a left-handed superhelix. Proc Natl Acad Sci USA 88:10148–10152

Ausubel FM, Brent R, Kingston RE, Moore DD, Seidman JG, Smith JA, Struhl K (1990) Current protocols in molecular biology. Green Publishing Associates and Wiley-Interscience, New York

Bohrmann B, Kellenberger E, Arnold-Schulz-Gahmen B, Sreenivas K, Suryanarayana T, Stroup D, Reeve JN (1994) Localization of histone-like proteins in thermophilic *Archaea* by immunogold electron microscopy. J Struct Biol 112:70–78

Crothers DM, Gartenberg MR, Shrader TE (1991) DNA bending in protein–DNA complexes. Methods Enzymol 208:118–146

Darcy TJ, Sandman KS, Reeve JN (1995) *Methanobacterium formicicum*, a mesophilic methanogen, contains three HFo histones. J Bacteriol 177:858–860

Dong F, van Holde KE (1991) Nucleosome positioning is determined by the $(H3–H4)_2$ tetramer. Proc Natl Acad Sci USA 88:10596–10600

Drew HR, Travers AA (1985) DNA bending and its relation to nucleosome positioning. J Mol Biol 186:773–790

Earle MJ, Abdur-Rashid A, Priestley ND (1996) Large scale synthesis of cyclodiphospho-D-glycerate. J Org Chem 61:5697–5700

Feliciello I, Chinali G (1993) A modified alkaline lysis method for the preparation of highly purified plasmid from *Escherichia coli*. Anal Biochem 212:394–401

Godde JS, Wolffe AP (1996) Nucleosome assembly on CTG triplet repeats. J Biol Chem 271:15222–15229

Grayling RA, Sandman K, Reeve JN (1994) Archaeal DNA binding proteins and chromosome structure. Syst Appl Microbiol 16:582–590

Grayling RA, Becktel WJ, Reeve JN (1995) Structure and stability of histone HMf from the hyperthermophilic archaeon *Methanothermus fervidus*. Biochemistry 34:8441–8448

Grayling RA, Sandman K, Reeve JN (1996a) DNA stability and DNA binding proteins. Adv Protein Chem 48:437–467

Grayling RA, Sandman K, Reeve JN (1996b) Histones and chromatin in hyperthermophilic *Archaea*. FEMS Microbiol Rev 18:203–213

Grunstein M (1990) Histone function in transcription. Annu Rev Cell Biol 6:563–678

Hamiche A, Carot V, Alilat M, De Lucia F, O'Donohue M-F, Révet B, Prunell A (1996) Interaction of the histones $(H3–H4)_2$ tetramer of the nucleosome with positively supercoiled DNA minicircles: Potential flipping of the protein from a left- to a right-handed superhelical form. Proc Natl Acad Sci USA 93:7588–7593

Hayes JJ, Clark DJ, Wolffe AP (1991) Histone contributions to the structure of DNA in the nucleosome. Proc Natl Acad Sci USA 88:6829–6833

Hensel R, König H (1988) Thermoadaptation of methanogenic bacteria by intracellular ion concentration. FEMS Microbiol Lett 49:75–79

Howard MT, Sandman K, Reeve JN, Griffith JD (1992) HMf, a histone-related protein from the hyperthermophilic archaeon *Methanothermus fervidus*, binds preferentially to DNA containing phased tracts of adenines. J Bacteriol 174:7864–7867

Kay R, McPherson J (1987) Hybrid pUC vectors for addition of new restriction enzyme sites to the ends of DNA fragments. Nucleic Acids Res 15:2778

Kim J, Zwieb C, Adhya S (1989) Bending of DNA by gene-regulatory proteins: construction and use of a DNA bending vector. Gene 85:15–23

Kornberg RD, Lorch Y (1992) Chromatin structure and transcription. Annu Rev Cell Biol 8:563–587

Meile L, Keiner A, Leisinger T (1983) A plasmid in the archaebacterium *Methanobacterium thermoautotrophicum*. Mol Gen Genet 191:480–484

Musgrave DR, Sandman KM, Reeve JN (1991) DNA binding by the archaeal histone HMf results in positive supercoiling. Proc Natl Acad Sci USA 88:10397–10401

Noll M (1974a) Subunit structure of chromatin. Nature 251:249–251

Noll M (1974b) Internal structure of the chromatin subunit. Nucleic Acids Res 1:1573–1578

Nölling J (1992) Mobile genetic elements in *Methanobacterium thermoformicicum*. PhD thesis. Wageningen Agricultural University, Wageningen, The Netherlands

Pruss D, Wolffe AP (1993) Histone–DNA contacts in the nucleosome core containing a *Xenopus* 5S rRNA gene. Biochemistry 32:6810–6814

Ramakrishnan V (1995) The histone fold: evolutionary questions. Proc Natl Acad Sci USA 92:11328–11330

Ronimus RS, Musgrave DR (1996) Purification and characterization of a histone-like protein from the archaeal isolate AN1, a member of the *Thermococcales*. Mol Microbiol 20:77–86

Sambrook J, Maniatis T, Fritsch EF (1989) Molecular cloning: a laboratory manual, 2nd edn. Cold Spring Harbor Laboratory Press, Plainview, NY

Sandman K, Krzycki JA, Dobrinski B, Lurz R, Reeve JN (1990) HMf, a DNA-binding protein isolated from the hyperthermophilic archaeon *Methanothermus fervidus*, is most closely related to histones. Proc Natl Acad Sci USA 87:5788–5791

Sandman K, Perler FB, Reeve JN (1994a) Histone-encoding genes from *Pyrococcus*: evidence for members of the HMf family of archaeal histones in a non-methanogenic archaeon. Gene 150:207–208

Sandman K, Grayling RA, Dobrinski B, Lurz R, Reeve JN (1994b) Growth-phase-dependent synthesis of histones in the archaeon *Methanothermus fervidus*. Proc Natl Acad Sci USA 91:12624–12628

Sandman K, Grayling RA, Reeve JN (1995) Improved N-terminal processing of recombinant proteins synthesized in *Escherichia coli*. Bio/Technology 13:504–506

Satchwell SC, Drew HR, Travers AA (1986) Sequence periodicities in chicken nucleosome core DNA. J Mol Biol 191:659–675

Shimizu M, Miyake M, Kanke F, Masumoto U, Shindo H (1995) Characterization of the binding of HU and IHF, homologous histone-like proteins of *Escherichia coli*, to curved and un-curved DNA. Biochim Biophys Acta 1264:330–336

Starich MR, Sandman K, Reeve JN, Summers MF (1996) NMR structure of HMfB from the hyperthermophile, *Methanothermus fervidus*, confirms that this archaeal protein is a histone. J Mol Biol 255:187–203

Stetter KO, Thomm M, Winter J, Wildgruber G, Huber H, Zillig W, Jane-Covic D, König H, Palm P, Wunderl S (1981) *Methanothermus fervidus*, sp. nov., a novel extremely thermophilic methanogen isolated from an Icelandic hot spring. Zentralbl Bakteriol Hyg I Abt Orig C2:166–178

Tan RK-Z, Prabhakaran M, Tung C-S, Harvey SC (1988) AUGUR: a program to predict, display and analyze the tertiary structure of B-DNA. Comput Appl Biosci 4:147–151

Thoma F (1992) Nucleosome positioning. Biochim Biophys Acta 1130:1–19

Thomas JO, Butler PJG (1978) The nucleosome core protein. Cold Spring Harbor Symp Quant Biol 42:119–125

Travers AA, Schwabe JWR (1993) Spurring on transcription? Curr Biol 3:898–900

Ulanovsky LE, Trifonov EN (1987) Estimation of wedge components in curved DNA. Nature 326:720–722

Wolffe A (1992) Chromatin: structure and function. Academic Press, San Diego

Wolffe A (1994) Transcription: in time with histones. Cell 77:13–16

Woodcock DM, Crowther PJ, Doherty J, Jefferson S, DeCruz E, Noyer-Weidner M, Smith SS, Michael MZ, Graham MW (1989) Quantitative evaluation of *Escherichia coli* host stains for tolerance to cytosine methylation in plasmid and phage recombinants. Nucleic Acids Res 17:3469–3478

Yanisch-Perron C, Vieira J, Messing J (1985) Improved M13 phage cloning vectors and host strains: nucleotide sequences of the M13mp18 and pUC19 vectors. Gene 33:103–119

Zwieb C, Kim J, Adhya S (1991) Detection of DNA bending by gel electrophoresis: use of plasmid vectors. In: Jost JP, Saluz HP (eds) A laboratory guide to in vitro studies of protein–DNA interactions. Birkhäuser, Boston, pp 245–254